Star formation rates measurements: linking stellar and dust emissions

Véronique Buat[1]

1. Aix-Marseille Université, CNRS, LAM (Laboratoire d'Astrophysique de Marseille) UMR7326, 13388, Marseille, France

Our knowledge of the cosmic mass assembly relies deeply on measurements of star formation rates as a function of redshift. Constraining the rate at which galaxies form stars across the Universe is of utmost importance if we want to understand galaxy formation and evolution. The star formation rate must be estimated robustly with a good knowledge of systematics. Combining stellar (ultraviolet) and dust (mid and far-IR) rest-frame emission is the best way to catch all the recent star formation activity.

1 Introduction

One of the most complex processes in galaxies is star formation and understanding it and its evolution with time remains a challenge for modern astronomy. The evolution of dark matter is now modeled with high accuracy and is shaping the large scale structures in the universe. The physics of baryons, including star formation, is much more difficult to understand and to implement in models of galaxy formation and evolution. The first natural step is to find constraints from observations by measuring a reliable star formation rate (SFR) at various scales and redshifts and studying the main drivers of its variation.

SFR and stellar masses ($M_{\rm star}$) are the main parameters estimated from large samples of galaxies. A large number of works found a tight relation between SFR and $M_{\rm star}$ both at low and high redshift often called the Main Sequence (MS) of galaxies (e.g. Noeske et al., 2007; Rodighiero et al., 2011, and reference therein). The slope and the scatter of this relation as well as its evolution with redshift put constraints on the star formation history of the galaxies as a function of their mass: the galaxies located on this MS may experience a rather smooth star formation evolution during several Gyr and the starburst mode seems to play a minor role in the production of stars in most of the galaxies (Rodighiero et al., 2011).

Major progress has been made in the study of the SFR inside the disk of nearby galaxies with a strong relation found between the SFR and the molecular gas content (e.g., Bigiel et al., 2008), and measurement of the star formation efficiency in galaxies is now possible up to large redshifts (e.g., Tacconi et al., 2013). Besides these studies aimed at understanding the process of star formation, the global amount of star formation in the universe is measured by building statistical samples with observables related to the recent star formation, a very popular result being the evolution of the star formation rate density with redshift (Madau & Dickinson, 2014, for a review).

2 General characteristics of star formation calibrations

Various calibrators are used, based on emissions known to be tightly linked to the population of young, massive stars: UV continuum, recombination lines, mid and far-infrared emission and radio continuum are the most popular markers of the recent star formation. The derivation of the SFR relies on conversion factors depending on the indicator used. In this section I will present the general way to derive the SFR from direct stellar emission and then discuss the uncertainties of the calibrations due to variations of the star formation histories. Very complete reviews about different star formation indicators were published recently (Kennicutt & Evans, 2012; Boissier, 2013).

2.1 Basic equation and standard calibrations

The fundamental equation to link the intrinsic luminosity emited by stars at wavelength λ and time t is

$$\mathrm{L}(\lambda, \mathrm{t}) = \int_0^{\mathrm{t}} \int_{\mathrm{M_{low}}}^{\mathrm{M_{up}}} \mathrm{F}_\lambda(\mathrm{m}, \theta)\mathrm{SFR}(\mathrm{t}-\theta)\psi(\mathrm{m})\ \mathrm{dm}\ \mathrm{d}\theta \tag{1}$$

where $\mathrm{F}_\lambda(\mathrm{m}, \theta)$ are the evolutionary stellar tracks, $\psi(m)$ the initial mass function, and $SFR(t)$ the star formation rate function. From this fundamental equation there are two ways to derive SFRs. One can use stellar populations synthesis models with various $SFR(t)$ to fit a large set of data at different wavelengths , the current SFR is an output parameter of the fit (with the stellar mass and other parameters depending on the specific code used), this method is particularly convenient when a large range of redshift is studied and when the wavelength coverage is wide. The method will be detailed in an other chapter of this volume. Another very popular way to proceed is to derive simple recipes. One assumes a SFR constant over a timescale T and the SFR becomes simply proportional to the luminosity integrated over T. The timescale T is chosen in order that the luminosity at wavelength λ reaches a steady state:

$$\mathrm{SFR} = \Big(\int_0^{\mathrm{t}} \int_{\mathrm{M_{low}}}^{\mathrm{M_{up}}} \mathrm{F}_\lambda(\mathrm{m}, \theta)\mathrm{SFR}(\mathrm{t}-\theta)\psi(\mathrm{m})\ \mathrm{dm}\ \mathrm{d}\theta\Big)^{-1} \times \mathrm{L}(\lambda) \tag{2}$$

The value of the conversion factor $C = SFR/L(\lambda)$ is calculated with a spectral synthesis code. The SFR calculated using a conversion factor can be different from the average of the star formation activity during T if the actual SFR is strongly varying during this period. The assumption of a constant SFR is likely to be valid on short timescales only and SFR should be derived from the emission of stars with short lifetimes, preferentially in the ultraviolet of for recombination lines of ionizing photons. The timescale to reach a steady state increases with wavelength from ~ 100 Myr in the UV to more than 1 Gyr in optical-near IR. The timescale found for ionizing photons (i.e. recombination lines) is of the order of few Myr (Kennicutt & Evans, 2012; Boissier, 2013). There is some evidence (see next subsection) for a SFR constant over few hundred Myrs, at least in the nearby universe: standard calibrations can be calculated, very popular ones being those of Kennicutt (1998). Note that the calibration depends also strongly on the initial mass function (e.g. Pflamm-Altenburg et al., 2009).

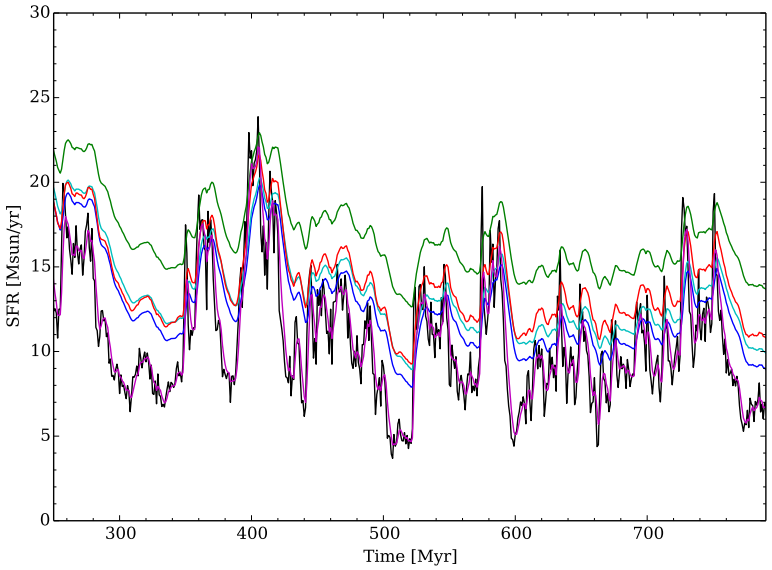

Fig. 1: SFR measurements for simulated galaxies from Fig. 3 of Boquien et al. (2014). The true SFR from simulations is shown in black. The SFRs measured with standard calibrators are plotted with coloured lines: magenta for the Lyman continuum, blue for the FUV (150 nm), cyan for the NUV (230 nm), green for the U band and red for the total infrared (IR) emission from dust, based on the assumption that the galaxy is entirely buried. Note that the true SFR and SFR from Lyman continuum are nearly blended.

2.2 Impact of a varying star formation rate

The assumption of a constant star formation rate is quite strong. It is very important to check that the condition is fulfilled before using standard calibrations. In the nearby universe the tight correlation found between the Hα and UV luminosity of large star forming galaxies is a strong argument in favor of a rather constant star formation rate over the typical timescale for the UV light to reach a steady state (i.e. $\sim$ 300 Myr) as illustrated in Fig. 2 of Hao et al. (2011). Conversely, nearby dwarf galaxies are likely to experiment rapid changes of their star formation rates (e.g., Weisz et al., 2012), implying variations in their Hα to UV flux ratio. Boquien et al. (2014) explore the impact of both long term and short term variability of the star formation history on the measurements of the SFR using classical estimators. Using simulations to model plausible star formations histories they find that, except for the Lyman continuum (and therefore recombination lines like the H_α one), classical estimators assuming a constant SFR over 100 Myr overestimate the true SFR as shown in Fig. 1. This effect is attributed to the long term variations of the SFR and to the contamination from stars living longer than the calibration timescale of 100 Myr. The authors suggest adopting SFR estimators calibrated over 1 Gyr rather than the commonly used 100 Myr to take this contamination into account. The Lyman continuum is by far the best tracer of the 'instantaneous' rate of star formation.

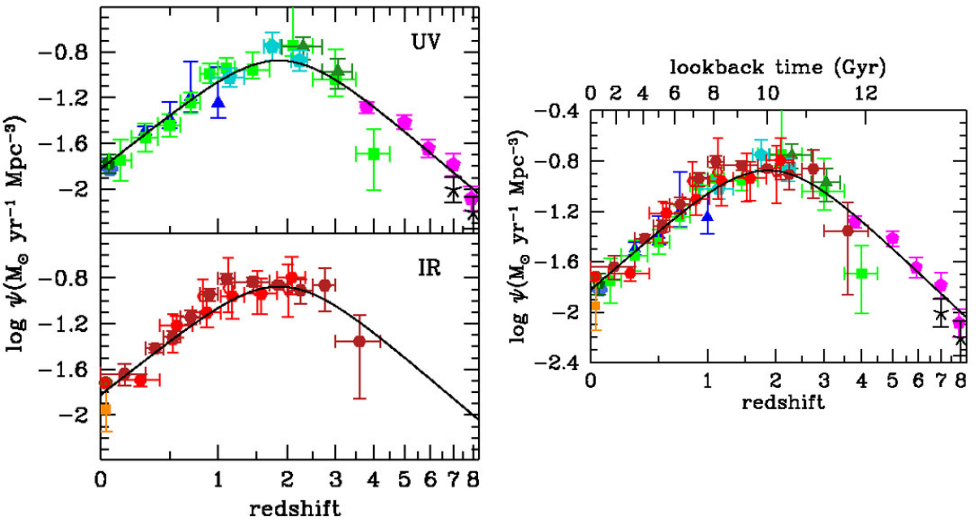

Fig. 2: SFR density measurements from UV and IR (left panel) , UV+IR (right panel) measurements, from Madau & Dickinson (2014). The IR measurements only sample redshifts lower than 3, beyond this limit only UV measurements are available, which are potentially affected by dust attenuation

3 Entering the real world: dust absorption and re-emission of stellar light

3.1 IR and composite star formation tracers

From the previous discussion it is quite natural to privilege the rest-frame UV emission to measure SFRs. The observations of the *GALEX* satellite up to $z = 1$ and the numerous optical surveys give very sensitive UV rest-frame measurements from the nearby universe to high redshifts and for large samples of galaxies (e.g., Salim et al., 2007; Cucciati et al., 2012). However, UV emission suffers from a major issue, which is dust attenuation. In the nearby universe and within galaxies like the Milky Way, about half of the stellar light is absorbed and re-emitted by dust at wavelengths larger than $\sim 5\mu$m, and that fraction can increase to more than 90% in starbursting objects. Therefore measuring the IR emission of galaxies has been identified as mandatory for measuring the total SFR, and adding both UV and IR emissions is now recognized as a very robust method to measure the SFR. As shown in Fig. 1 both emissions exhibit similar temporal variations, confirming that they trace the star formation activity both visible (UV) and hidden by dust (IR). Some calibrations combine different wavelengths and account for all the star formation directly observed in UV-optical or reprocessed in thermal IR (e.g. Kennicutt & Evans, 2012, and references therein).

The development of IR facilities allows the building of statistical samples of galaxies detected in IR, although the lower sensitivity of IR detectors combined with poor spatial resolution makes comparison with UV-optical surveys still difficult. The *Spitzer* and *Herschel* deep observations combined with ground-based optical surveys give us a complete view of the star formation up to $z \sim 2$. The very high redshifts ($z >> 2$) remain almost unexplored in IR even with *Herschel* (Madau & Dickinson, 2014, see Fig. 2) and stacking methods are intensively used to find the average IR

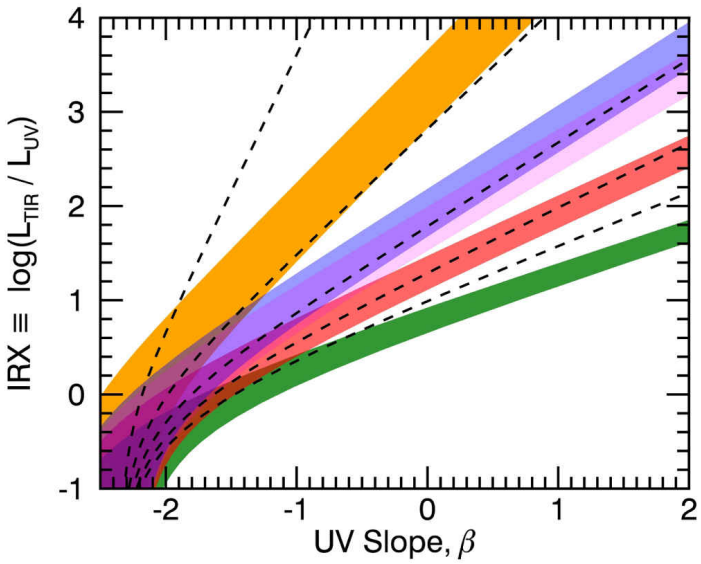

Fig. 3: Predicted relations between $L_{\rm IR}/L_{\rm UV}$ and the UV slope β for different attenuation recipes. The colored areas from top to left correspond to the Milky Way extinction curve, the starburst law, the MOSDEF law, and two SMC extinction curves. Dashed lines to modified starburst laws with different slopes (Salmon et al., 2016, their Fig.4 and references therein)

emission of optically faint objects not detected individually (e.g., Heinis et al., 2013).

3.2 Dust attenuation corrections

When dust emission is measured, accurate star formation rates can be derived by combining IR and UV data as described above , but these data are often not available, in particular for deep optical surveys. As a consequence, it is particularly important to study the dependence of dust attenuation on parameters such as the observed luminosity, the stellar mass, or the slope of the UV continuum, since it could be used to correct large samples for the effect of dust attenuation, at least in a statistical way. The global amount of dust attenuation is robustly estimated by comparing dust and stellar emission, through the $L_{\rm IR}/L_{\rm UV}$ ratio (e.g. Buat et al., 2005). When IR data are not available, the shape of the UV continuum (< 3000) has been proposed as a proxy to measure the amount of attenuation. D. Calzetti, G. Meurer and collaborators have shown that the UV continuum of local starburst galaxies can be fitted by a power law ($f_\lambda(\mathrm{erg\ cm^{-2}s^{-1}nm^{-1}}) \propto \lambda^\beta$) for $\lambda > 120$ nm. β correlates with the amount of dust attenuation measured by $L_{\rm IR}/L_{\rm UV}$ – see Calzetti (2001) for a review). This local starburst relation is widely used to estimate dust attenuation in galaxies although the universal validity of the relation is questioned (e.g. Casey et al., 2014). Actually the relation between $L_{\rm IR}/L_{\rm UV}$ and β is expected to depend on both the star formation history (e.g. Kong et al., 2004) and dust attenuation characteristics, as illustrated in Fig.3 from the recent work of Salmon et al. (2016). The attenuation recipe has also some impact in the determination of stellar masses (Lo Faro et al., submitted).

Dust attenuation is also found to be correlated with the stellar mass, as already reported from the local universe up to high redshifts, and the relation does not seem to

evolve with redshift (Heinis et al., 2014; Bernhard et al., 2014; Whitaker et al., 2014). Recently it has been proposed to use rest-frame colors to predict the amount of dust attenuation; the universality of such relations still has to be investigated (Arnouts et al., 2013; Forrest et al., 2016)

4 The reliability of SFR measurements: confrontation with simulated catalogues

The comparison of the observed and simulated spectral energy distributions of galaxies inform us which fitting method provides the correct galaxy parameters. Properties of mock galaxies are known *a priori* by definition, and using their simulated emission helps us to understand the effectiveness of the assumptions made to derive the SFR, even though there is no guarantee that the simulated galaxies have star formation histories similar to real ones in the Universe. Simulated catalogues are either the outputs of hydrodynamical or semi-analytical codes, or generated from real catalogues and simple assumptions to reproduce the observed SEDs (e.g. Wuyts et al., 2009; Pforr et al., 2012; Boquien et al., 2014; Ciesla et al., 2015). These studies have shown that it is very difficult to reconstruct the whole star formation history, and the true stellar age of stellar populations is underestimated because of the outshining of the young populations in star-forming galaxies, with obvious effects on stellar mass determinations (e.g. Pforr et al., 2012). The difficulty of reproducing realistic star formation histories with simple modelling is illustrated in Fig. 3 from the work of Ciesla et al. (2015). If dust attenuation is well constrained with IR data the recent star formation rates are well reproduced (Buat et al., 2014).

5 Conclusions

We have seen that recipes used to measure star formation rates are based on strong assumptions about the recent star formation history: most of the time a constant star formation rate over at least 100 Myr. In fact this seems to be too short a timescale to account for older stars which also contribute to the stellar emission, even in the UV. Very short term variations of the star formation rate (< 10 Myr) are only detectable with the measurement of the ionizing flux through recombination lines. Because of the impact of dust attenuation the UV light alone, without any correction, cannot be used to measure the star formation rate of galaxies. The most robust method consists of combining UV (stellar) and IR (dust) emissions. In the absence of IR data, some relations can be used to infer the amount of dust attenuation, but these relations must be used with caution and their validity checked carefully before using them.

References

Arnouts, S., et al., *Encoding of the infrared excess in the NUVrK color diagram for star-forming galaxies*, A&A **558**, A67 (2013), 1309.0008

Bernhard, E., et al., *Modelling the connection between ultraviolet and infrared galaxy populations across cosmic times*, MNRAS **442**, 509 (2014), 1405.1425

Bigiel, F., et al., *The Star Formation Law in Nearby Galaxies on Sub-Kpc Scales*, AJ **136**, 2846 (2008), 0810.2541

Boissier, S., *Star Formation in Galaxies*, in T. D. Oswalt, W. C. Keel (eds.) Planets, Stars and Stellar Systems. Volume 6: Extragalactic Astronomy and Cosmology, 141 (2013)

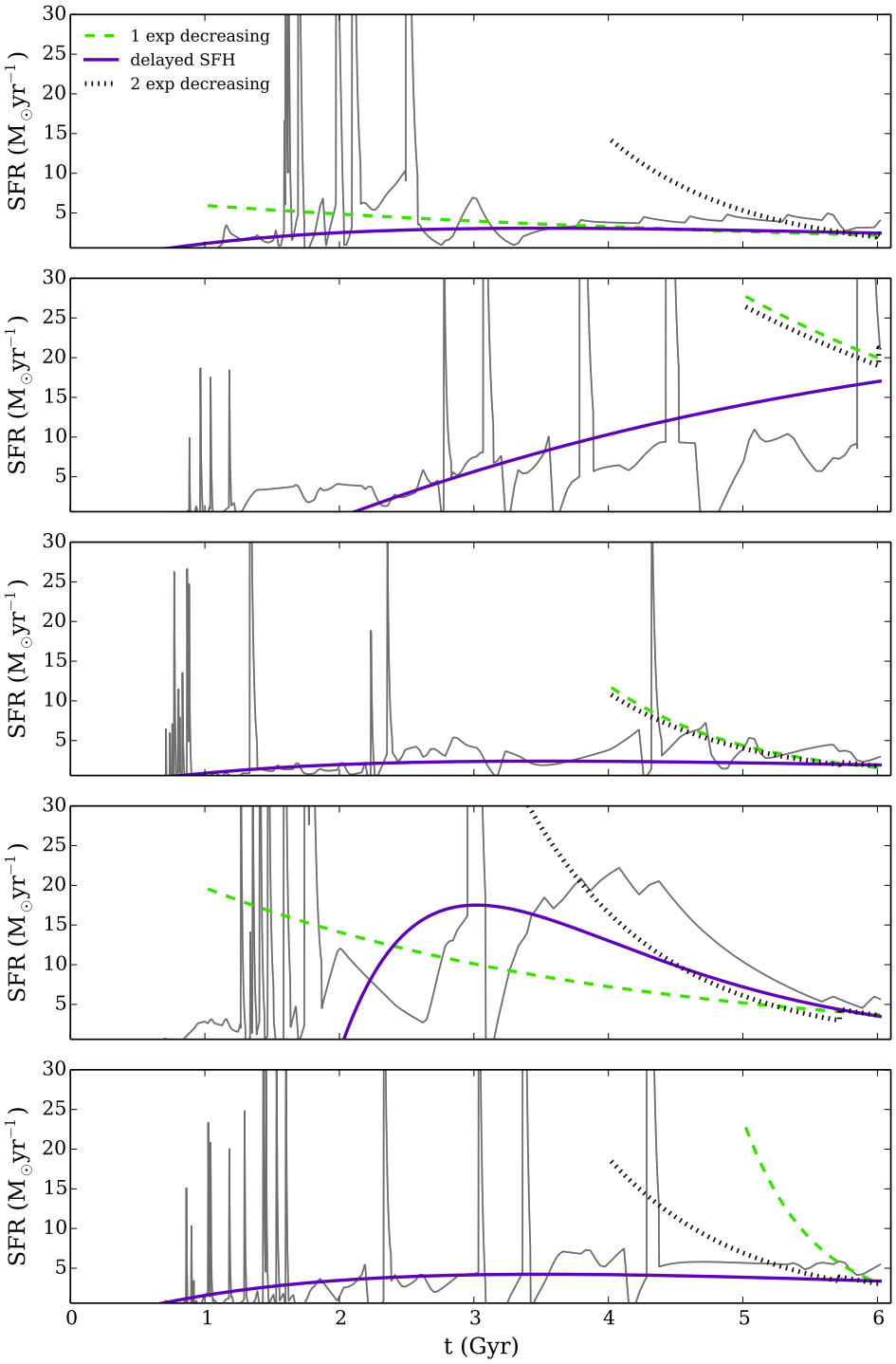

Fig. 4: Star formation histories from semi-analytical modelling (black line) and the corresponding best fits obtained with the code CIGALE and 3 different models of star formation (Ciesla et al., 2015, their Fig.7)

Boquien, M., Buat, V., Perret, V., *Impact of star formation history on the measurement of star formation rates*, A&A **571**, A72 (2014), 1409.5792

Buat, V., et al., *Dust Attenuation in the Nearby Universe: A Comparison between Galaxies Selected in the Ultraviolet and in the Far-Infrared*, ApJ **619**, L51 (2005), astro-ph/0411343

Buat, V., et al., *Ultraviolet to infrared emission of $z > 1$ galaxies: Can we derive reliable star formation rates and stellar masses?*, A&A **561**, A39 (2014), 1310.7712

Calzetti, D., *The Dust Opacity of Star-forming Galaxies*, PASP **113**, 1449 (2001), astro-ph/0109035

Casey, C. M., et al., *Are Dusty Galaxies Blue? Insights on UV Attenuation from Dust-selected Galaxies*, ApJ **796**, 95 (2014), 1410.0702

Ciesla, L., et al., *Constraining the properties of AGN host galaxies with spectral energy distribution modelling*, A&A **576**, A10 (2015), 1501.03672

Cucciati, O., et al., *The star formation rate density and dust attenuation evolution over 12 Gyr with the VVDS surveys*, A&A **539**, A31 (2012), 1109.1005

Forrest, B., et al., *UV to IR Luminosities and Dust Attenuation Determined from ˜4000 K-selected Galaxies at $1 < z < 3$ in the ZFOURGE Survey*, ApJ **818**, L26 (2016), 1602.01096

Hao, C.-N., et al., *Dust-corrected Star Formation Rates of Galaxies. II. Combinations of Ultraviolet and Infrared Tracers*, ApJ **741**, 124 (2011), 1108.2837

Heinis, S., et al., *HERMES: unveiling obscured star formation - the far-infrared luminosity function of ultraviolet-selected galaxies at $z = 1.5$*, MNRAS **429**, 1113 (2013), 1211.4336

Heinis, S., et al., *HerMES: dust attenuation and star formation activity in ultraviolet-selected samples from z=4 to 1.5*, MNRAS **437**, 1268 (2014), 1310.3227

Kennicutt, R. C., Evans, N. J., *Star Formation in the Milky Way and Nearby Galaxies*, ARA&A **50**, 531 (2012), 1204.3552

Kennicutt, R. C., Jr., *Star Formation in Galaxies Along the Hubble Sequence*, ARA&A **36**, 189 (1998), astro-ph/9807187

Kong, X., Charlot, S., Brinchmann, J., Fall, S. M., *Star formation history and dust content of galaxies drawn from ultraviolet surveys*, MNRAS **349**, 769 (2004), astro-ph/0312474

Madau, P., Dickinson, M., *Cosmic Star-Formation History*, ARA&A **52**, 415 (2014), 1403.0007

Noeske, K. G., et al., *Star Formation in AEGIS Field Galaxies since z=1.1: The Dominance of Gradually Declining Star Formation, and the Main Sequence of Star-forming Galaxies*, ApJ **660**, L43 (2007), astro-ph/0701924

Pflamm-Altenburg, J., Weidner, C., Kroupa, P., *Diverging UV and Hα fluxes of star-forming galaxies predicted by the IGIMF theory*, MNRAS **395**, 394 (2009), 0901.4335

Pforr, J., Maraston, C., Tonini, C., *Recovering galaxy stellar population properties from broad-band spectral energy distribution fitting*, MNRAS **422**, 3285 (2012), 1203.3548

Rodighiero, G., et al., *The Lesser Role of Starbursts in Star Formation at $z = 2$*, ApJ **739**, L40 (2011), 1108.0933

Salim, S., et al., *UV Star Formation Rates in the Local Universe*, ApJS **173**, 267 (2007), 0704.3611

Salmon, B., et al., *Breaking the Curve with CANDELS: A Bayesian Approach to Reveal the Non-Universality of the Dust-Attenuation Law at High Redshift*, ApJ **827**, 20 (2016), 1512.05396

Tacconi, L. J., et al., *Phibss: Molecular Gas Content and Scaling Relations in z ˜ 1-3 Massive, Main-sequence Star-forming Galaxies*, ApJ **768**, 74 (2013), 1211.5743

Weisz, D. R., et al., *Modeling the Effects of Star Formation Histories on Hα and Ultraviolet Fluxes in nearby Dwarf Galaxies*, ApJ **744**, 44 (2012), 1109.2905

Whitaker, K. E., et al., *Constraining the Low-mass Slope of the Star Formation Sequence at 0.5 < z <2.5*, ApJ **795**, 104 (2014), 1407.1843

Wuyts, S., et al., *Recovering Stellar Population Properties and Redshifts from Broadband Photometry of Simulated Galaxies: Lessons for SED Modeling*, ApJ **696**, 348 (2009), 0901.4337